Supporting Online Material for

Brain Evolution Triggers Increased Diversification of Electric Fishes

Bruce A. Carlson,* Saad M. Hasan, Michael Hollmann, Derek B. Miller, Luke J. Harmon, Matthew E. Arnegard

*To whom correspondence should be addressed. E-mail: carlson.bruce@wustl.edu

Published 29 April 2011, *Science* **332**, 583 (2011)
DOI: 10.1126/science.1201524

This PDF file includes:

Materials and Methods

Phylogenetic Reconstruction

A sound phylogenetic framework is required to understand patterns of brain evolution and how they relate to the diversification of signals and species. Mormyrids have already been well studied phylogenetically (*2-6, 8, 31-37*). Our purpose in the present analysis was not to extend this phylogenetic literature. Rather, our aim was to estimate a single phylogeny, including all relevant species in the best-sampled communities, for making a formal comparison of rates of signal divergence and species diversification between mormyrid lineages (see below). Thus, we used published *cytb* sequences from the mormyrid assemblage of the Ivindo River basin near Makokou, Gabon (*2, 3, 34*) (aligned sequences provided by J. P. Sullivan) and from the petrocephaline assemblage of Odzala National Park in the Lékoli River basin, Republic of the Congo (*5, 6*) (aligned sequences provided by S. Lavoué). In the case of the Odzala petrocephaline assemblage, we only considered the most common *cytb* haplotype for every species, each of which appears to be exclusively monophyletic with respect to all other sympatric species (*5, 6*). To these focal species we added published *cytb* sequences for the outgroup species, *Gymnarchus niloticus* (*3*) (aquarium specimen), and a specimen of *Myomyrus macrops* collected by J. P. Sullivan from the Ubangi River, Central African Republic (*2*). Table S1 lists the specimen numbers and GenBank accession numbers for all specimens used to construct the phylogeny.

We conducted a Bayesian phylogenetic analysis on the matrix of aligned *cytb* sequences using MrBayes ver. 3.1.2 (*38, 39*) and the GTR+Γ model of sequence evolution: i.e., a general time reversible model with nucleotide substitution rate variation assumed to follow a gamma distribution. The Metropolis-coupled, Markov chain Monte Carlo (MCMCMC) process included four chains, three heated and one cold. Starting from random trees, we simultaneously performed two independent Bayesian analyses (runs) for 2,000,000 generations each. We were confident that stationarity had been reached by this stopping point because the standard deviation of split frequencies had dropped to 0.006. During the parallel runs, we sampled parameter values and trees every 100 generations. Log-likelihood values for the sampled trees stabilized by 100,000 generations into each run. Therefore, we only used the last 1,900,000 generations in both runs to estimate the 50% majority-rule consensus tree and clade credibility values (i.e., posterior probabilities, 'PP'). The consensus tree (Fig. 1) was computed using all 38,000 trees pooled across the two Bayesian runs. Although the monophyly of the Petrocephalinae appears rather weakly supported in the consensus tree (PP = 0.52; see Fig. 1), the monophyly of this group and its sister-clade relationship to the Mormyrinae are strongly supported by morphological synapomorphies (*21*) and phylogenetic analysis using whole mitogenome sequences (*40*). The phylogeny provides robust support for the monophyly of 'clade A', the focus of the current study (PP = 1.00; see Fig. 1), in agreement with several existing phylogenies based on multiple molecular markers (*2-6, 32, 34, 37*).

Next, we pruned the Ivindo River *Petrocephalus microphthalmus* specimen from the tree, leaving the *P. microphthalmus* specimen collected in Odzala (this is the only species with more than one representative in our phylogeny; see Fig. 1). Using the penalized likelihood routine in the program r8s ver. 1.71 (*41, 42*), we converted the consensus

Bayesian tree to ultrametric form. We selected a smoothing parameter ($\log_{10}\lambda = 2.2$) using cross-validation and ran the penalized likelihood procedure, checking the stability of the solution using the 'checkgradient' command in r8s. All analyses of signal divergence and species diversification (below) were conducted on this ultrametric tree. When taxa were not included in an analysis, we simply pruned them from this ultrametric tree, which served as the single phylogenetic framework for subsequent tests of signal divergence and species diversification rates.

Brain Histology

We obtained fixed brains in one of three ways: (1) laboratory specimens – after anesthesia in 300 mg/l MS-222, each fish was perfused through the heart with Hickman's Ringer, followed by 4% paraformaldehyde in 0.1 M phosphate buffer (e.g. *Brienomyrus brachyistius* in Fig. 2A and *Petrocephalus soudanensis* in Fig. 2B); (2) freshly caught field specimens – after anesthesia in 300 mg/l MS-222, the skull was opened, followed by immersion fixation in 4% paraformaldehyde in 0.1 M phosphate buffer (e.g. *Petrocephalus microphthalmus* in Fig. 2A); (3) specimens donated by the Cornell University Museum of Vertebrates – brains were removed from curated specimens, which had been fixed in 10% phosphate-buffered formalin for approximately two weeks and subsequently stored in 70% ethanol (e.g. *Myomyrus macrops* in Fig. 2B). In each case, we post-fixed brains in 4% paraformaldehyde in 0.1 M phosphate buffer for several days, then embedded them in gelatin and post-fixed them overnight before slicing. We obtained 50 μm horizontal sections with a vibrating microtome. Sections were mounted on chrom-alum subbed slides, stained with cresyl violet, dehydrated in a graded alcohol series, cleared with xylene, and then coverslipped (*43*).

The exterolateral nucleus (EL) was clearly identified in each brain based on topology (*10, 12, 44-50*), which is largely considered the single-most important criterion for establishing the homology of brain regions (*51-53*). Previous anatomical studies of EL in three clade A species describe separate anterior and posterior subdivisions that are clearly divisible based on cytology; these are referred to as ELa and ELp, respectively (*10, 12, 44-50*). As described in the main text, some of the species we studied fit this previous description, while other species have just a single, small EL lacking any subdivisions (Fig. 2); we refer to these two phenotypes as ELa/ELp and EL, respectively. Evoked potential recordings from the ELa/ELp of *P. microphthalmus* reveal 2-3 ms latency responses to electrosensory stimulation that are blocked at short delays following the electric discharge motor command, exactly as described for species in clade A (*48, 50, 54-56*). This further satisfies the following additional criteria for establishing homology (*51, 57*): physiological properties, connectivity (input from knollenorgans via the nucleus of the electrosensory lateral line lobe, or nELL; see fig. S1), and function (detection of electric signals generated by other fish). For each brain, we delineated the borders of EL or ELa/ELp in each section based on cytology (*12, 44-47*). We then determined the total volume of EL or ELa/ELp by summing cross-sectional areas, multiplying by section thickness, and taking the mean of the left and right sides (no lateral asymmetries were detected). We normalized this value by total brain mass, determined after post-fixing and before embedding. No apparent differences in the architecture or normalized volumes of these brain regions were observed between the

brains of closely-related specimens obtained through different fixation methods. A full list of species for which we obtained EL anatomy data is provided in table S2.

Electroreceptor Histology

Curated specimens donated by the Cornell University Museum of Vertebrates had been fixed in 10% phosphate-buffered formalin for approximately two weeks before storage in 70% ethanol. Laboratory specimens were fixed in 70% ethanol. Mormyrids have three distinct types of electroreceptors: ampullary organs used for passive electrolocation, mormyromasts used for active electrolocation, and knollenorgans used for electric communication (*18, 20*). There is a semi-transparent layer of skin that covers the body where these receptors are located. In fixed specimens, this skin layer turns white and is easily removed. We photographed specimens before removing this layer in pieces. We then placed each piece in a solution of 0.05% toluidine blue for 10 minutes, followed by three 5-minute washes in 70% ethanol. The three different types of electroreceptors could then be visually identified and distinguished under a microscope (fig. S2A). We mapped the location of knollenorgans in each piece of skin onto the original photograph, and then outlined the specimen (Fig. 3; fig. S2B, C). A full list of species for which we obtained data on knollenorgan distributions is provided in table S2.

Behavioral Playback Experiments

Playback experiments were performed on fish caught in Gabon near Lebamba (2°12′0″ S, 11°30′0″ E) and Lambaréné (0°41′18″ S, 10°13′55″ E) during July-August 2009. Methods for collecting mormyrids and recording electric signals have been described in detail elsewhere (*16, 34, 58, 59*). For studying clade A, we focused our efforts on *Paramormyrops kingsleyae*, a species that is widely distributed throughout Gabon; however, we also performed experiments on small numbers of additional clade A species (see Fig. 4A). For studying outgroup species, we focused on the four petrocephaline species found in Gabon (*21*). For obtaining playback signals, we recorded from individuals placed in water taken from the collection site (conductivity = 10-30 μS/cm; temperature = 22-26 °C). Using Ag/AgCl electrodes, electric signals were amplified using a bandwidth of 0.0001-50 kHz (CWE, Inc. BMA-200), analog-to-digital converted at 97.6 kHz (24-bit Sigma-Delta converter; Tucker-Davis Technologies RM1), and then saved to disk using custom software written in Matlab 2007a (The MathWorks, Inc.).

For playback experiments, each fish was placed in a rectangular PVC enclosure (3.5 x 3.5 x 20 cm) with Ag/AgCl stimulus electrodes spanning the length of both sides of the middle of the inside of the enclosure, and Ag/AgCl recording electrodes at each end (fig. S3A). Stimuli were digital-to-analog converted at 48.8 kHz (Tucker-Davis Technologies RM1) and isolated from ground (A-M Systems, Inc. model 2200). The output of the fish was amplified (CWE, Inc. BMA-200) and digitized at 48.8 kHz (Tucker-Davis Technologies RM1). Custom software written in Matlab 2007a was used to deliver stimuli and time-stamp the fish's electric discharges.

For stimuli, we used electric signal waveforms recorded from conspecifics, as well as conspecific waveforms that were distorted by making a 90º phase-shift (fig. S3B). The latter involves advancing the phase angles of the power spectrum by 90º for all positive frequencies and retarding the phase angles by 90º for all negative frequencies, resulting in

a temporally distorted signal waveform with a frequency spectrum and total energy equivalent to the original waveform (*13, 60*). Stimulus trains consisted of 10 bursts of 10 pulses each, with an intra-burst interval of 30 ms, inter-burst interval of 10 s, and peak-to-peak intensity of 145 mV/cm. For control stimulation, all 100 pulses were an identical conspecific waveform. Experimental stimuli were the same, except that all 10 pulses in the 9th burst were a phase-shifted version of the same conspecific waveform (fig. S3C). Each playback used a stimulus waveform recorded from a different conspecific (*61*).

In species that responded to stimulation with increases in discharge rate, we determined the maximum discharge rates in response to each of the 10 bursts after Gaussian smoothing (fig. S4A). In species that responded to stimulation by pausing, we determined the duration of pauses in response to each of the 10 bursts (fig. S4B). Discrimination was assessed as the change in maximum discharge rate or change in pause duration from the 8th to 9th bursts (Fig. 4A).

Analysis of Signal Divergence Rates

To study broad patterns of signal evolution in the Mormyridae, we focused on the most intensively studied assemblages of clade A species and petrocephaline species: i.e., the mormyrid assemblage of the Ivindo River basin (*3*) and the petrocephaline assemblage of Odzala National Park (*5, 6*). The Ivindo assemblage is dominated by numerous clade A species but also contains three petrocephaline species. In contrast, the Odzala assemblage contains a high diversity of both clade A and petrocephaline species, although the available molecular phylogenetic data for this assemblage only include the eleven petrocephaline species known from Odzala. These two communities represent the most diverse assemblages of clade A and Petrocephalinae, respectively, documented thus far from any region of Africa (*3, 5, 6, 9, 62*). The numerous high quality electric signal recordings and fine-scale biogeographical data collected for these assemblages are unrivalled by any other mormyrid community that has been investigated previously. Our comparison of signal divergence rates used previously published signal waveforms recorded from these two assemblages (*3, 5, 6*) (fig. S5).

We performed cross-correlation between all 407 signal waveforms in the dataset (*63*). We used the maximum of the absolute value of cross-correlation coefficients as a pair-wise measure of waveform similarity (fig. S6). The absolute value was chosen since waveform polarity is a variable feature that depends on the relative orientations of sender and receiver (*16, 64*). This resulted in a matrix of pair-wise similarities ranging from 0 (no similarity) to 1 (identical waveforms). A phenotypic space describing signal variation was then constructed by applying multidimensional scaling (MDS) to this similarity matrix using the function ‘mdscale’ with Kruskal's normalized stress1 criterion in Matlab 2007a (Fig. 4B). MDS is an ordination technique that projects similarities or distances in some character or variable onto an N-dimensional coordinate space to maximally recreate all pair-wise distances (*65*). The degree of correspondence between the pair-wise distances in the input matrix relative to the MDS map is represented by stress, which can range from 0 (perfect correspondence) to 1 (no correspondence). In our MDS analysis we set N = 2, which resulted in a stress of 0.0635. Based on coordinate data for the two resulting MDS axes, we computed the pair-wise Mahalanobis D^2 between the centroids of each species/morph distribution using the function ‘mahalanobis’ in the program R ver. 2.9.2 (*66, 67*). Since sample sizes were low for some species, we calculated D^2 using

a pooled within-species variance-covariance matrix (*3*). We then plotted D^2 against patristic distances taken from the ultrametric tree for all clade A pair-wise comparisons and all other pair-wise comparisons outside this clade. Patristic distances were scaled to a maximum of 1.0. This plot allowed us to visualize the pattern of accumulation of signal differences across distances in the phylogenetic tree without assuming any model of trait evolution *a priori* (*3*). For clarity, we refer to D^2 as 'signal waveform distance' and patristic distance as 'phylogenetic distance' in Fig. 4C. We also computed D^2 by calculating separate pooled variance-covariance matrices for all clade A species and all other species. This resulted in the same pattern of more rapid signal evolution in clade A (data not shown).

We used Brownie ver. 2.1.1 to statistically compare rates of accumulation of signal waveform disparity between clade A and all outgroup mormyrids in a Brownian motion framework by means of maximum likelihood (*24*). The Brownian motion rate parameter (σ^2) describes the rate with which trait variance among species has increased over evolutionary time. Using a censored rate test, we compared a model that fit a single σ^2 across the entire ultrametric tree of mormyrid relationships to a two-rate model allowing clade A and all other mormyrids to differ in σ^2. This comparison was made separately for each MDS-derived axis of signal variation. Given the moderate number of taxa under consideration, we made each comparison using the small-sample-size-corrected version of the Akaike Information Criterion (AICc) and a likelihood ratio test evaluated with a parametric bootstrapping procedure (5,000 pseudoreplicates). These model evaluation approaches avoid the inflated Type 1 errors that stem from using the χ^2 distribution with small sample sizes (*24, 68*).

Analysis of Species Diversification Rates

We analyzed species diversification rates using the approach described by Rabosky et al. (*25*) (table S3). This method is appropriate when one has an incompletely sampled phylogenetic tree with branch lengths. We assigned missing species to lineages with representatives in the tree using a combination of phylogenetic and taxonomic data, so that we could account for the total diversity of each group. Net diversification rate (r) is defined in the standard way as $r = \lambda - \mu$, where λ = rate of speciation and μ = rate of extinction. We then compared a model with constant r across the tree to one where the focal clade A was allowed to have a different net diversification rate (r_A) from the rest of the tree (r_{other}). We compared the fit of these two nested models using a likelihood-ratio test. Given our small dataset and the difficulty in estimating extinction rates from comparative data (*69*), we set the relative extinction fraction to $\varepsilon = \mu / \lambda$ rather than attempting to estimate it from the data (*70*). We repeated our analyses using a range of ε values (ε = 0, 0.5, 0.9, and 0.99) (*25*). Across this range of assumed ε, we found statistical support for net diversification rates that are 3-5 times higher in clade A than in closely-related out-group lineages (table S3). Patterns of species richness in sub-lineages contained within clade A suggest that this increase in diversification immediately followed the origin of clade A rather than arising more recently during its radiation. For instance, the first extant lineage to split from the rest of clade A (*Mormyrops* spp.) is a species-rich genus (21 extant species) with high signal waveform diversity (*2, 4, 7, 58*).

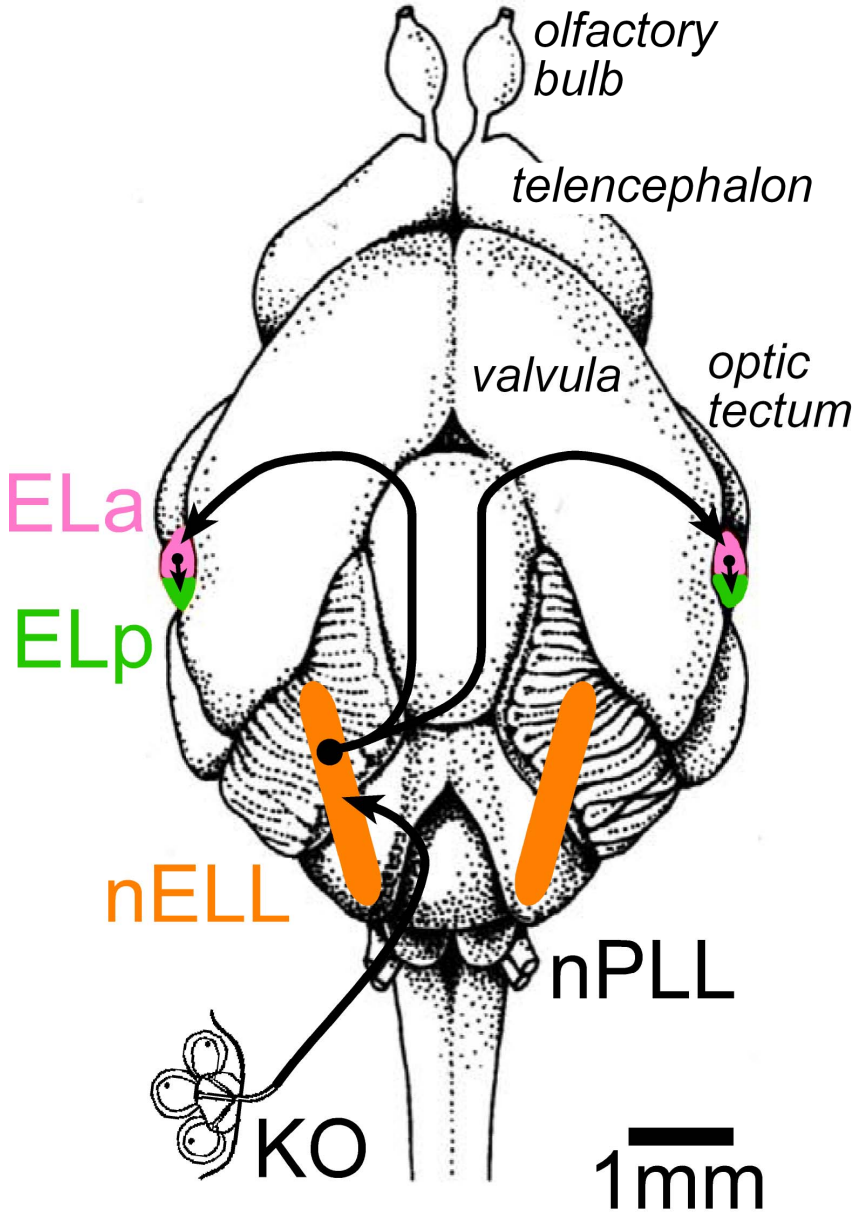

Fig. S1. Dorsal view of the brain of the clade A species *Brienomyrus brachyistius*, highlighting the knollenorgan electrosensory pathway. Knollenorgan (KO) primary afferent fibers project ipsilaterally to the nucleus of the electrosensory lateral line lobe (nELL) in the hindbrain via the anterior (not shown) and posterior lateral line nerves (nPLL). Neurons in the nELL project bilaterally to the anterior exterolateral nucleus (ELa) in the midbrain, which in turn projects ipsilaterally to the adjacent posterior exterolateral nucleus (ELp).

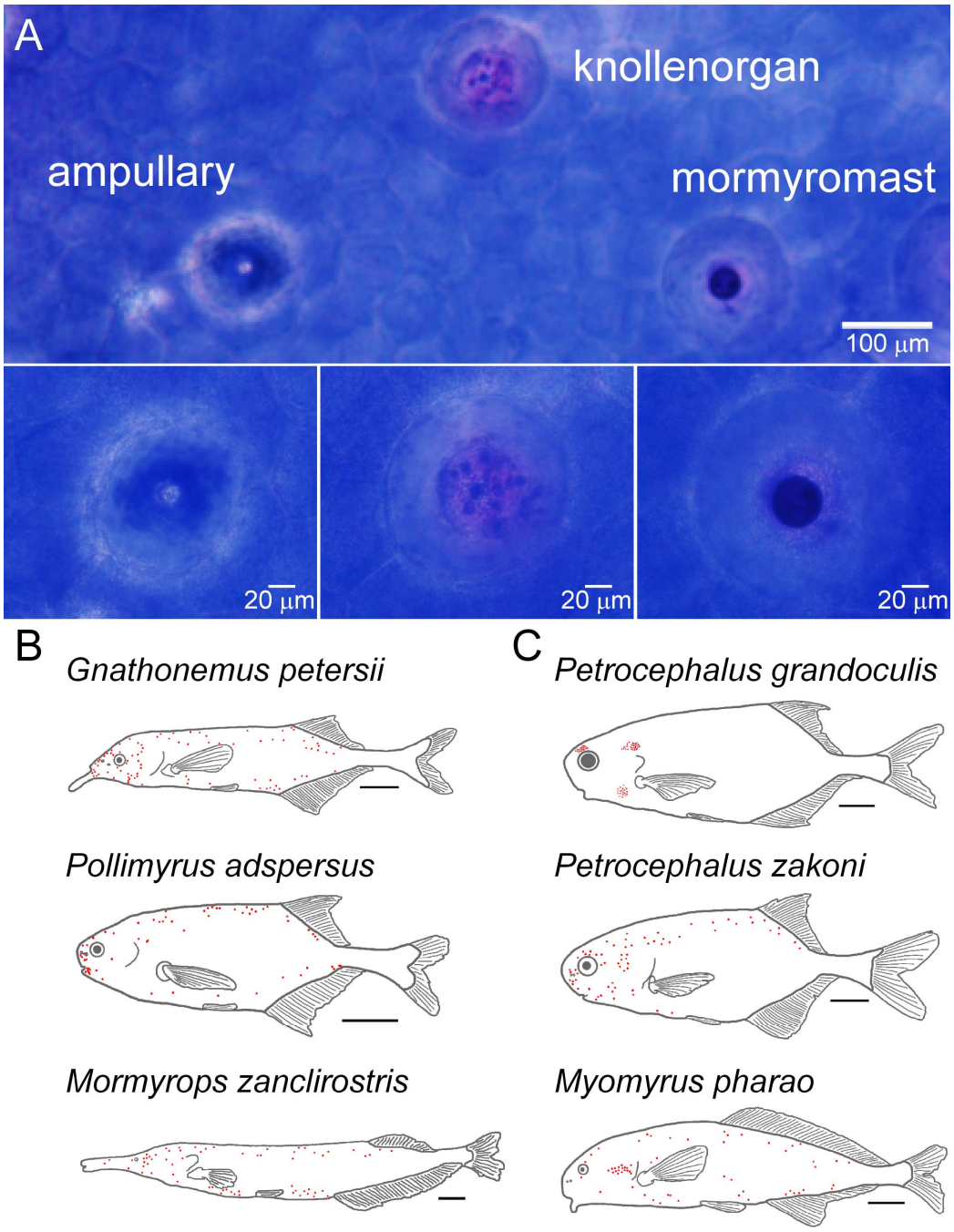

Fig. S2. Mapping of knollenorgan electroreceptor locations. (A) Portion of skin from the clade A species *Brienomyrus brachyistius* stained with toluidine blue. Knollenorgans can easily be distinguished from ampullary and mormyromast electroreceptors. (B) Maps of knollenorgan locations from three species in clade A. (C) Maps of knollenorgan locations from three species outside of clade A. Knollenorgan locations are indicated by red dots. Scale bars = 1 cm.

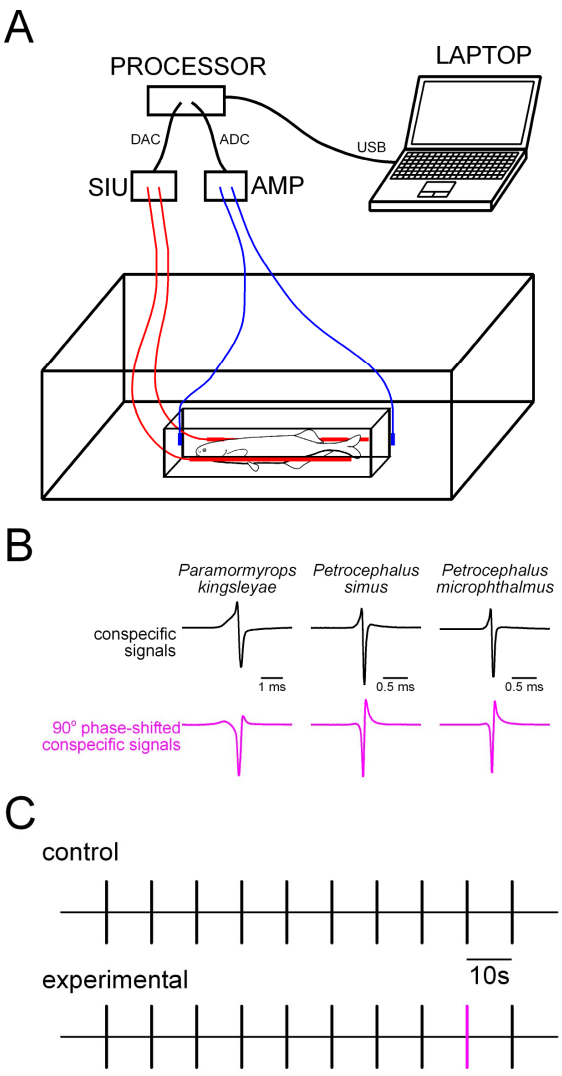

Fig. S3. Behavioral discrimination experiments. (A) Set-up for field playback experiments. Each fish was placed in a rectangular PVC enclosure with stimulus electrodes spanning the length of both sides of the inside of the enclosure (red) and recording electrodes at each end (blue). Stimuli were generated on a laptop and delivered through the digital-to-analog converter (DAC) of a USB-connected portable processor. Stimuli were isolated from ground prior to delivery (SIU). The output of the fish was amplified (AMP), then digitized by the analog-to-digital converter (ADC) of the processor. (B) Examples of stimulus waveforms used in experiments for three species. Conspecific signals were recorded in the field. These waveforms were temporally distorted by phase-shifting them by 90º. (C) Two types of stimulus trains were used. Control stimulus trains consisted of 10 bursts of 10 pulses each; each pulse was an identical conspecific waveform. Experimental stimulus trains were the same except that the 9th burst of pulses consisted of phase-shifted versions of the same conspecific waveform.

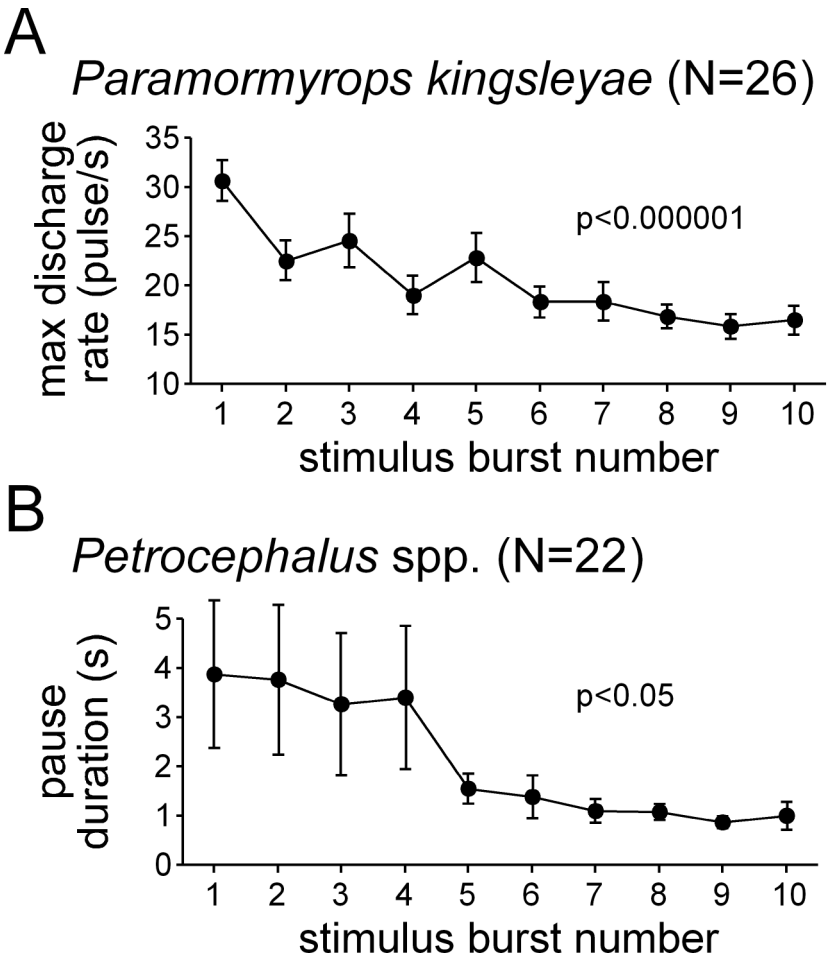

Fig. S4. Habituation of behavioral responses to electrosensory stimulation. (A) In *Paramormyops kingsleyae*, stimulation resulted in bursts of electrical output, quantified as the maximum discharge rate after Gaussian smoothing. This response habituates throughout the course of control stimulus trains. (B) In all four petrocephaline species, *Petrocephalus balayi* (N = 1), *P. microphthalmus* (N = 10), *P. simus* (N = 7), and *P. sullivani* (N = 4), stimulation elicited pauses in electrical output, quantified as pause duration. This response also habituates throughout the course of control stimulus trains. Values show the mean ± s.e.m. Statistical significance of the decrease in response with repeated stimulus presentations was assessed using repeated-measures ANOVA.

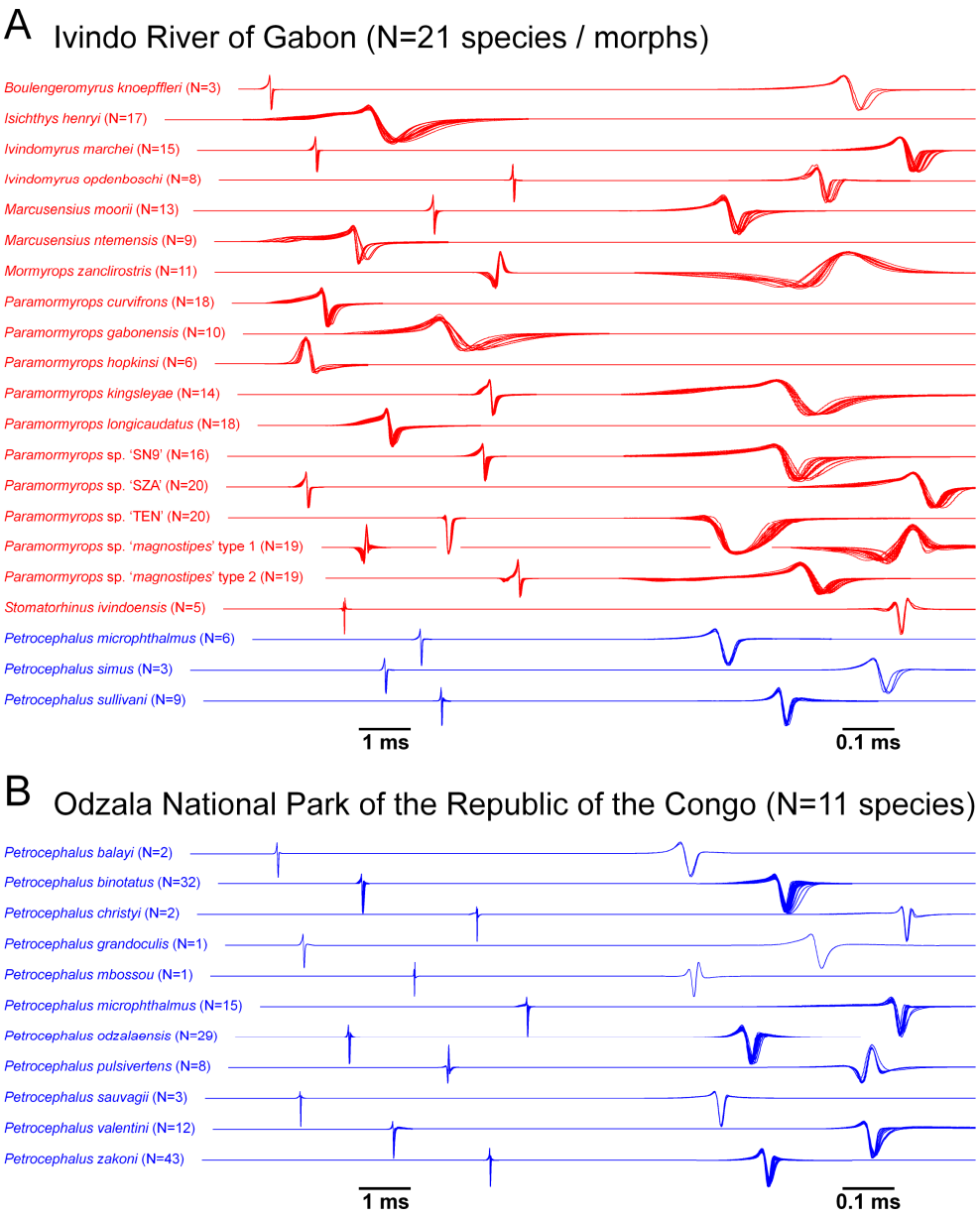

Fig. S5. Electric signal waveforms used for analyzing rates of signal evolution. (A) Waveforms from the Ivindo mormyrid assemblage of Gabon (*3*). (B) Waveforms from the petrocephaline assemblage of Odzala National Park in the Republic of the Congo (*5*, *6*). Species from clade A are shown in red, all other species are shown in blue. In each case, waveforms are amplitude-normalized and plotted head-positive up. Multiple waveforms from different individuals of the same species are superimposed and aligned to the head-positive peak (except for *Paramormyrops* sp. 'TEN', for which waveforms are aligned to the head-negative peak). The left and right columns show waveforms at two different timescales (1 ms and 0.1 ms scale bars, respectively). The longest waveforms are shown only in the left column.

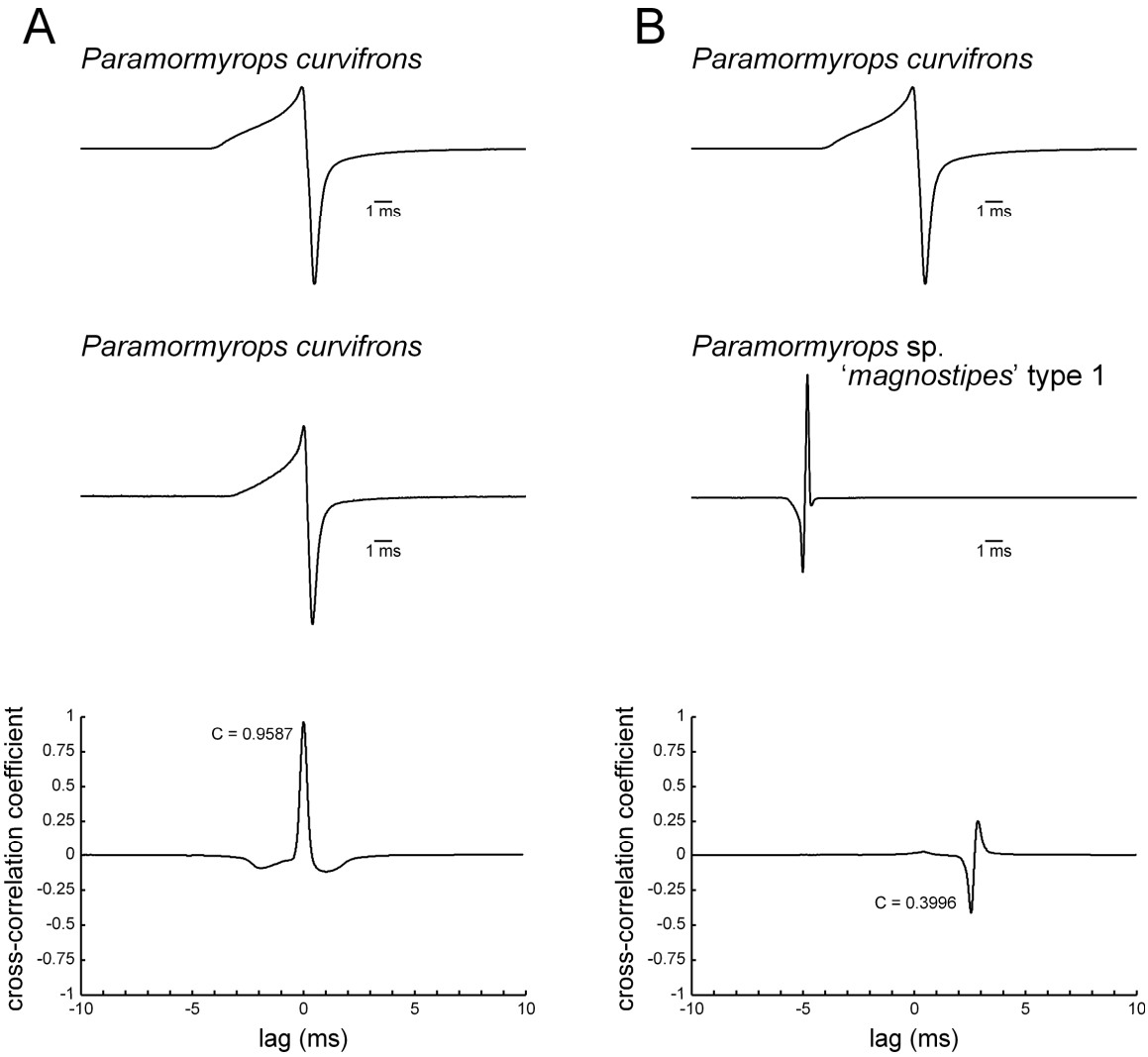

Fig. S6. Cross-correlation method used to measure waveform similarity. (A) Example showing the cross-correlation of two conspecific waveforms recorded from different individuals of *Paramormyrops curvifrons*. The cross-correlation coefficients (bottom) reveal the correlation between the two waveforms as a function of the relative delay (lag) between them. The maximum of the absolute values of this function (C = 0.9587) provides a scalar measure of waveform similarity. (B) Example showing the cross-correlation of two heterospecific waveforms (*P. curvifrons* and *Paramormyrops* sp. '*magnostipes*' type 1). Here the waveforms are less similar (C = 0.3996).

Table S1. Cytochrome b (*cytb*) sequences used for estimating mormyrid phylogeny, showing corresponding specimen information. Museum catalog numbers preceded by 'CU' are specimens housed in the Cornell University Museum of Vertebrates, Ithaca, NY. The single museum catalog number preceded by 'AMNH' is a specimen housed in the American Museum of Natural History, New York, NY.

Taxon	Museum catalog no., specimen no.	Collection site	GenBank accession no.
Paramormyrops sp. type 1	CU 78326, #2297	Loa Loa Rapids, Ivindo River, Gabon	AF477452
Paramormyrops sp. type 2	CU 78344, #2295	Loa Loa Rapids, Ivindo River, Gabon	AF477455
Paramormyrops sp. 'TEN'	CU 80809, #2011	Bialé Stream, Ivindo R. basin, Gabon	AF477453
Paramormyrops curvifrons	CU 81661, #2050	Loa Loa Rapids, Ivindo River, Gabon	AF477469
Paramormyrops longicaudatus	CU 78355, #2289	Loa Loa Rapids, Ivindo River, Gabon	AF201576
Paramormyrops kingsleyae	CU 80816, #2116	Bialé Stream, Ivindo R. basin, Gabon	AF477466
Paramormyrops sp. 'SN9'	CU 89360, #5552	Loa Loa Rapids, Ivindo River, Gabon	FJ830628
Paramormyrops hopkinsi	CU 78352, #2285	Loa Loa Rapids, Ivindo River, Gabon	AF201575
Paramormyrops gabonensis	CU 79702, #2048	Loa Loa Rapids, Ivindo River, Gabon	AF201603
Paramormyrops sp. 'SZA'	CU 80848, #2008	Bialé Stream, Ivindo R. basin, Gabon	AF477475
Marcusenius ntemensis	CU 79706, #2186	Loa Loa Rapids, Ivindo River, Gabon	AF201593
Boulengeromyrus knoepffleri	CU 79692, #2248	Loa Loa Rapids, Ivindo River, Gabon	AF201573
Ivindomyrus opdenboschi	CU 84642, #2106	Loa Loa Rapids, Ivindo River, Gabon	DQ166689
Ivindomyrus marchei	CU 81642, #2183	Loa Loa Rapids, Ivindo River, Gabon	DQ166677
Stomatorhinus ivindoensis	CU 70703, #2074	Bialé Stream, Ivindo R. basin, Gabon	AF201612
Marcusenius moorii	CU 79697, #2013	Balé Creek, Ivindo R. basin, Gabon	AF201595
Isichthys henryi	CU 79705, #2179	Loa Loa Rapids, Ivindo River, Gabon	AF201590
Mormyrops zanclirostris	CU 79707, #2210	Makokou region, Ivindo River, Gabon	AF201599
Myomyrus macrops	AMNH 228166, #2524	Ubangi River, Congo R. basin, Central African Republic	AF201602
Petrocephalus simus	CU 79701, #2035	Balé Creek, Ivindo R. basin, Gabon	AF201604
Petrocephalus sullivani	CU 79700, #2038	Balé Creek, Ivindo R. basin, Gabon	AF201606
Petrocephalus valentini	CU 88058, #5175	Lékoli River, Congo R. basin, Congo	EU770181
Petrocephalus sauvagii	CU 87864, #5206	Lékoli River, Congo R. basin, Congo	EU770160
Petrocephalus pulsivertens	CU 88097, #5263	Lékoli River, Congo R. basin, Congo	EU770174
Petrocephalus christyi	CU 88095, #5261	Lékoli River, Congo R. basin, Congo	EU770183
Petrocephalus mbossou	CU 92389, #6183	Lékoli River, Congo R. basin, Congo	EU770163
Petrocephalus grandoculis	CU 92385, #6181	Lékoli River, Congo R. basin, Congo	EU770155
Petrocephalus zakoni	CU 92391, #6132	Lékoli River, Congo R. basin, Congo	EU770170
Petrocephalus binotatus	CU 88064, #5001	Lékoli River, Congo R. basin, Congo	EU770164
Petrocephalus balayi	CU 88111, #5314	Lékoli River, Congo R. basin, Congo	EU770192
Petrocephalus odzalaensis	CU 87852, #5148	Lékoli River, Congo R. basin, Congo	EU770156
Petrocephalus microphthalmus	CU 82208, #2199	Loa Loa Rapids, Ivindo River, Gabon	EU770185
Petrocephalus microphthalmus	CU 87940, #5092	Lékoli River, Congo R. basin, Congo	EU770188
Gymnarchus niloticus	CU 80334, no spec. #	Aquarium import	AF201586

Table S2. Specimens used for studying brain anatomy and knollenorgan distributions. Taxonomic assignments are based on our cytochrome b (*cytb*) phylogeny (Fig. 1) as well as several published studies (*2-6, 32, 34, 37, 58*).

Sub-family		Genus	Species[1]	EL anatomy sample size	Pattern of EL organization[2]	Knollenorgan distribution[3]
Mormyrinae	Clade A	*Brevimyrus*	*niger*			B[4]
		Brienomyrus	*brachyistius*	5	ELa/ELp	B
		Campylomormyrus	*numenius*	1	ELa/ELp	
			rhynchophorus			B[4]
			tamandua	1	ELa/ELp	B
		Gnathonemus	*petersii*	1	ELa/ELp	B
		Isichthys	*henryi*	2	ELa/ELp	
		Ivindomyrus	*marchei*	2	ELa/ELp	
		Marcusenius	*moorii*	2	ELa/ELp	B[4]
			senegalensis			B[4]
		Mormyrops	*nigricans*	1	ELa/ELp	B[4]
			zanclirostris	2	ELa/ELp	B
		Mormyrus	*caballus*			B[4]
		Paramormyrops	*gabonensis*	2	ELa/ELp	
			longicaudatus	1	ELa/ELp	
			sp. 'BON'	1	ELa/ELp	
			sp. 'VAD'	1	ELa/ELp	
		Pollimyrus	*adspersus*	2	ELa/ELp	B
		Stomatorhinus	*walkeri*	3	ELa/ELp	
	Myomyrus		*macrops*	1	EL	C-B
			pharao	1	EL	C-B
Petrocephalinae	*Petrocephalus*		*balayi*	1	EL	C[4]
			binotatus			C[4]
			christyi			C[4]
			grandoculis	1	EL	C
			microphthalmus	3	ELa/ELp	B
			odzalaensis			C[4]
			pulsivertens	1	EL	C
			sauvagii			C[4]
			simus	4	EL	C
			soudanensis	4	EL	C
			sullivani	2	EL	C
			valentini	1	EL	C
			zakoni	3	EL	B

1. Undescribed species are referred to by established 3-letter cheironyms (*34, 59*).
2. 'EL' = relatively small exterolateral nucleus; 'ELa/ELp' = relatively large exterolateral nucleus divided into anterior and posterior subdivisions.
3. 'B' = broad distribution of knollenorgan receptors throughout the head and trunk; 'C' = distinct clusters of knollenorgan receptors on the head; 'C-B' = intermediate pattern with one cluster of knollenorgan receptors on the head as well as a broad distribution of knollenorgan receptors at relatively low density.
4. Knollenorgan distributions based on published studies (*6, 20, 21*). These previous studies used visual examination of intact specimens rather than the staining method employed in the current study.

Table S3. Model comparisons testing for a shift in diversification rate in clade A relative to other mormyrids. We set the relative extinction fractions (ε) to different values, and then compared a model with constant net diversification rate (r) across the tree to one with different net diversification rates for clade A (r_A) and the rest of the tree (r_{other}).

Model	Parameter estimates	r_A/r_{other}	lnL	Delta	*p*-value
ε = 0					
Single rate	r=0.0079		-95.1		
Two rate	r_{other}=0.0032, r_A=0.0100	3.12	-84.0	22.2	<0.001
ε = 0.5					
Single rate	r=0.0062		-92.7		
Two rate	r_{other}=0.0025, r_A=0.0083	3.32	-84.1	17.1	<0.001
ε = 0.9					
Single rate	r=0.0030		-90.1		
Two rate	r_{other}=0.0010, r_A=0.0042	4.20	-85.7	8.8	0.003
ε = 0.99					
Single rate	r=0.0005		-90.5		
Two rate	r_{other}=0.00014, r_A=0.00073	5.21	-88.1	4.8	0.03

References and Notes

1. C. J. Hoskin, M. Higgie, Speciation via species interactions: The divergence of mating traits within species. *Ecol. Lett.* **13**, 409 (2010).

2. J. P. Sullivan, S. Lavoué, C. D. Hopkins, Molecular systematics of the African electric fishes (Mormyroidea: teleostei) and a model for the evolution of their electric organs. *J. Exp. Biol.* **203**, 665 (2000).

3. M. E. Arnegard *et al*., Sexual signal evolution outpaces ecological divergence during electric fish species radiation. *Am. Nat.* **176**, 335 (2010).

4. S. Lavoué, J. P. Sullivan, C. D. Hopkins, Phylogenetic utility of the first two introns of the S7 ribosomal protein gene in African electric fishes (Mormyroidea: Teleostei) and congruence with other molecular markers. *Biol. J. Linn. Soc. Lond.* **78**, 273 (2003).

5. S. Lavoué, M. E. Arnegard, J. P. Sullivan, C. D. Hopkins, *Petrocephalus* of Odzala offer insights into evolutionary patterns of signal diversification in the Mormyridae, a family of weakly electrogenic fishes from Africa. *J. Physiol. Paris* **102**, 322 (2008).

6. S. Lavoué, J. P. Sullivan, African weakly electric fishes of the genus *Petrocephalus* (Osteoglossomorpha: Mormyridae) of Odzala National Park, Republic of the Congo (Lékoli River, Congo River basin) with description of five new species. M. E. Arnegard, *Zootaxa* **2600**, 1 (2010).

7. W. N. Eschmeyer, J. D. Fong, *Catalog of Fishes* (California Academy of Sciences, San Francisco, 2010).

8. P. G. D. Feulner, F. Kirschbaum, V. Mamonekene, V. Ketmaier, R. Tiedemann, Adaptive radiation in African weakly electric fish (Teleostei: Mormyridae: *Campylomormyrus*): A combined molecular and morphological approach. *J. Evol. Biol.* **20**, 403 (2007).

9. C. D. Hopkins, On the diversity of electric signals in a community of mormyrid electric fish in west Africa. *Am. Zool.* **21**, 211 (1981).

10. M. A. Xu-Friedman, C. D. Hopkins, Central mechanisms of temporal analysis in the knollenorgan pathway of mormyrid electric fish. *J. Exp. Biol.* **202**, 1311 (1999).

11. B. A. Carlson, in *Communication in Fishes*, F. Ladich, S. P. Collin, P. Moller, B. G. Kapoor, Eds. (Science Publishers, Enfield, NH, 2006), vol. 2, pp. 805-848.

12. C. C. Bell, T. Szabo, in *Electroreception*, T. H. Bullock, W. Heiligenberg, Eds. (John Wiley & Sons, New York, 1986), pp. 375-421.

13. C. D. Hopkins, A. H. Bass, Temporal coding of species recognition signals in an electric fish. *Science* **212**, 85 (1981).

14. P. G. D. Feulner, M. Plath, J. Engelmann, F. Kirschbaum, R. Tiedemann, Electrifying love: Electric fish use species-specific discharge for mate recognition. *Biol. Lett.* **5**, 225 (2009).

15. P. Machnik, B. Kramer, Female choice by electric pulse duration: Attractiveness of the males' communication signal assessed by female bulldog fish, *Marcusenius pongolensis* (Mormyridae, Teleostei). *J. Exp. Biol.* **211**, 1969 (2008).

16. M. E. Arnegard, B. S. Jackson, C. D. Hopkins, Time-domain signal divergence and discrimination without receptor modification in sympatric morphs of electric fishes. *J. Exp. Biol.* **209**, 2182 (2006).

17. A. H. Bass, in *Electroreception*, T. H. Bullock, W. Heiligenberg, Eds. (Wiley, New York, 1986), pp. 13–70.

18. H. H. Zakon, in *Electroreception*, T. H. Bullock, W. Heiligenberg, Eds. (Wiley, New York, 1986), pp. 103–156.

19. A. H. Bass, C. D. Hopkins, Comparative aspects of brain organization of an African "wave" electric fish, *Gymnarchus niloticus*. *J. Morphol.* **174**, 313 (1982).

20. W. Harder, Die Beziehungen zwischen Elektrorezeptoren, Elektrischem Organ, Seitenlinienorganen und Nervensystem bei den Mormyridae (Teleostei, Pisces). *Z. Vgl. Physiol.* **59**, 272 (1968).

21. S. Lavoué, C. D. Hopkins, A. K. Toham, The *Petrocephalus* (Pisces, Osteoglossomorpha, Mormyridae) of Gabon, Central Africa, with the description of a new species. *Zoosystema* **26**, 511 (2004).

22. N. Post, G. von der Emde, The "novelty response" in an electric fish: Response properties and habituation. *Physiol. Behav.* **68**, 115 (1999).

23. P. Moller, J. Serrier, D. Bowling, electric organ discharge displays during social encounter in the weakly electric fish *Brienomyrus niger* L. (Mormyridae). *Ethology* **82**, 177 (1989).

24. B. C. O'Meara, C. Ané, M. J. Sanderson, P. C. Wainwright, Testing for different rates of continuous trait evolution using likelihood. *Evolution* **60**, 922 (2006).

25. D. L. Rabosky, S. C. Donnellan, A. L. Talaba, I. J. Lovette, Exceptional among-lineage variation in diversification rates during the radiation of Australia's most diverse vertebrate clade. *Proc. Biol. Sci.* **274**, 2915 (2007).

26. M. J. Ryan, Neuroanatomy influences speciation rates among anurans. *Proc. Natl. Acad. Sci. U.S.A.* **83**, 1379 (1986).

27. O. Seehausen *et al*., Speciation through sensory drive in cichlid fish. *Nature* **455**, 620 (2008).

28. Y. Terai *et al*., Divergent selection on opsins drives incipient speciation in Lake Victoria cichlids. *PLoS Biol.* **4**, e433 (2006).

29. J. B. Sylvester *et al*., Brain diversity evolves via differences in patterning. *Proc. Natl. Acad. Sci. U.S.A.* **107**, 9718 (2010).

30. C. A. Shumway, Habitat complexity, brain, and behavior. *Brain Behav. Evol.* **72**, 123 (2008).

31. J. Alves-Gomes, C. D. Hopkins, Molecular insights into the phylogeny of mormyriform fishes and the evolution of their electric organs. *Brain Behav. Evol.* **49**, 324 (1997).

32. S. Lavoué, R. Bigorne, G. Lecointre, J.-F. Agnèse, Phylogenetic relationships of mormyrid electric fishes (Mormyridae; Teleostei) inferred from cytochrome b sequences. *Mol. Phylogenet. Evol.* **14**, 1 (2000).

33. S. Lavoué, J. P. Sullivan, M. E. Arnegard, C. D. Hopkins, Differentiation of morphology, genetics and electric signals in a region of sympatry between sister species of African electric fish (Mormyridae). *J. Evol. Biol.* **21**, 1030 (2008).

34. J. P. Sullivan, S. Lavoué, C. D. Hopkins, Discovery and phylogenetic analysis of a riverine species flock of African electric fishes (Mormyridae: Teleostei). *Evolution* **56**, 597 (2002).

35. J. P. Sullivan, S. Lavoué, M. E. Arnegard, C. D. Hopkins, AFLPs resolve phylogeny and reveal mitochondrial introgression within a species flock of African electric fish (Mormyroidea: Teleostei). *Evolution* **58**, 825 (2004).

36. P. G. D. Feulner, F. Kirschbaum, R. Tiedemann, Adaptive radiation in the Congo River: An ecological speciation scenario for African weakly electric fish (Teleostei; Mormyridae; *Campylomormyrus*). *J. Physiol. Paris* **102**, 340 (2008).

37. M. E. Arnegard, D. J. Zwickl, Y. Lu, H. H. Zakon, Old gene duplication facilitates origin and diversification of an innovative communication system—twice. *Proc. Natl. Acad. Sci. U.S.A.* **107**, 22172 (2010).

38. J. P. Huelsenbeck, F. Ronquist, MRBAYES: Bayesian inference of phylogenetic trees. *Bioinformatics* **17**, 754 (2001).

39. F. Ronquist, J. P. Huelsenbeck, MrBayes 3: Bayesian phylogenetic inference under mixed models. *Bioinformatics* **19**, 1572 (2003).

40. S. Lavoué *et al*., Remarkable morphological stasis in an extant vertebrate despite tens of millions of years of divergence. *Proc. Biol. Sci.* **278**, 1003 (2011).

41. M. J. Sanderson, Estimating absolute rates of molecular evolution and divergence times: A penalized likelihood approach. *Mol. Biol. Evol.* **19**, 101 (2002).

42. M. J. Sanderson, r8s: Inferring absolute rates of molecular evolution and divergence times in the absence of a molecular clock. *Bioinformatics* **19**, 301 (2003).

43. B. A. Carlson, Neuroanatomy of the mormyrid electromotor control system. *J. Comp. Neurol.* **454**, 440 (2002).

44. F. Haugedé-Carré, The mesencephalic exterolateral posterior nucleus of the mormyrid fish *Brienomyrus niger*: Efferent connections studied by the HRP method. *Brain Res.* **178**, 179 (1979).

45. E. Mugnaini, L. Maler, Cytology and immunocytochemistry of the nucleus extrolateralis anterior of the mormyrid brain: Possible role of GABAergic synapses in temporal analysis. *Anat. Embryol. (Berl.)* **176**, 313 (1987).

46. M. A. Friedman, M. Kawasaki, Calretinin-like immunoreactivity in mormyrid and gymnarchid electrosensory and electromotor systems. *J. Comp. Neurol.* **387**, 341 (1997).

47. M. A. Friedman, C. D. Hopkins, Neural substrates for species recognition in the time-coding electrosensory pathway of mormyrid electric fish. *J. Neurosci.* **18**, 1171 (1998).

48. B. A. Carlson, Temporal-pattern recognition by single neurons in a sensory pathway devoted to social communication behavior. *J. Neurosci.* **29**, 9417 (2009).

49. S. Amagai, M. A. Friedman, C. D. Hopkins, Time coding in the midbrain of mormyrid electric fish. I. Physiology and anatomy of cells in the nucleus exterolateralis pars anterior. *J. Comp. Physiol. A Neuroethol. Sens. Neural Behav. Physiol.* **182**, 115 (1998).

50. S. Amagai, Time coding in the midbrain of mormyrid electric fish. II. Stimulus selectivity in the nucleus exterolateralis pars posterior. *J. Comp. Physiol. A Neuroethol. Sens. Neural Behav. Physiol.* **182**, 131 (1998).

51. G. F. Striedter, *Principles of Brain Evolution* (Sinauer, Sunderland, MA, 2005).

52. R. Nieuwenhuys, Comparative neuroanatomy: Place, principles, practice and programme. *Eur. J. Morphol.* **32**, 142 (1994).

53. L. Puelles, L. Medina, Field homology as a way to reconcile genetic and developmental variability with adult homology. *Brain Res. Bull.* **57**, 243 (2002).

54. P. S. Enger, S. Libouban, T. Szabo, Fast conducting electrosensory pathway in the mormyrid fish, *Gnathonemus petersii*. *Neurosci. Lett.* **2**, 133 (1976).

55. C. J. Russell, C. C. Bell, Neuronal responses to electrosensory input in mormyrid valvula cerebelli. *J. Neurophysiol.* **41**, 1495 (1978).

56. T. Szabo, P. S. Enger, S. Libouban, Electrosensory systems in the mormyrid fish, *Gnathonemus petersii*: Special emphasis on the fast conducting pathway. *J. Physiol. (Paris)* **75**, 409 (1979).

57. C. B. G. Campbell, W. Hodos, The concept of homology and the evolution of the nervous system. *Brain Behav. Evol.* **3**, 353 (1970).

58. C. D. Hopkins, S. Lavoué, J. P. Sullivan, in *The Fresh and Brackish Water Fishes of Lower Guinea*, West-Central Africa, M. L. J. Stiassny, G. G. Teugels, C. D.

Hopkins, Eds. (IRD, Publications scientifiques du Muséum, MRAC, Paris, 2007), vol. 1.

59. M. E. Arnegard, S. M. Bogdanowicz, C. D. Hopkins, Multiple cases of striking genetic similarity between alternate electric fish signal morphs in sympatry. *Evolution* **59**, 324 (2005).

60. W. Heiligenberg, R. A. Altes, Phase sensitivity in electroreception. *Science* **199**, 1001 (1978).

61. D. Kroodsma, Suggested experimental designs for song playbacks. *Anim. Behav.* **37**, 600 (1989).

62. C. D. Hopkins, Design features for electric communication. *J. Exp. Biol.* **202**, 1217 (1999).

63. C. Chatfield, *The Analysis of Time Series: An Introduction*. (Chapman and Hall, New York, 2004).

64. C. D. Hopkins, Temporal structure of non-propagated electric communication signals. *Brain Behav. Evol.* **28**, 43 (1986).

65. J. B. Kruskal, M. Wish, *Multidimensional Scaling*. (Sage, Beverly Hills, CA, 1978).

66. P. Mahalanobis, On the generalized distance in statistics. *Proc. Natl. Inst. Sci. India* **2**, 49 (1936).

67. N. Eldredge *et al*., The dynamics of evolutionary stasis. *Paleobiology* **31**, (suppl), 133 (2005).

68. S. A. Price *et al*., Functional innovations and morphological diversification in parrotfish. *Evolution* **64**, 3057 (2010).

69. D. L. Rabosky, Extinction rates should not be estimated from molecular phylogenies. *Evolution* **64**, 1816 (2010).

70. M. E. Alfaro *et al*., Nine exceptional radiations plus high turnover explain species diversity in jawed vertebrates. *Proc. Natl. Acad. Sci. U.S.A.* **106**, 13410 (2009).

Acknowledgments: We thank C. D. Hopkins and J. R. Gallant for help with field work, J. P. Friel (Cornell University Museum of Vertebrates) for providing specimens, and S. Lavoué and J. P. Sullivan for providing *cytb* sequences (GenBank accession numbers provided in table S1). Supported by NSF IOS-0818390 (B.A.C.); L.J.H. was supported by NSF DEB-0919499.